**SUPPORTING INFORMATION**

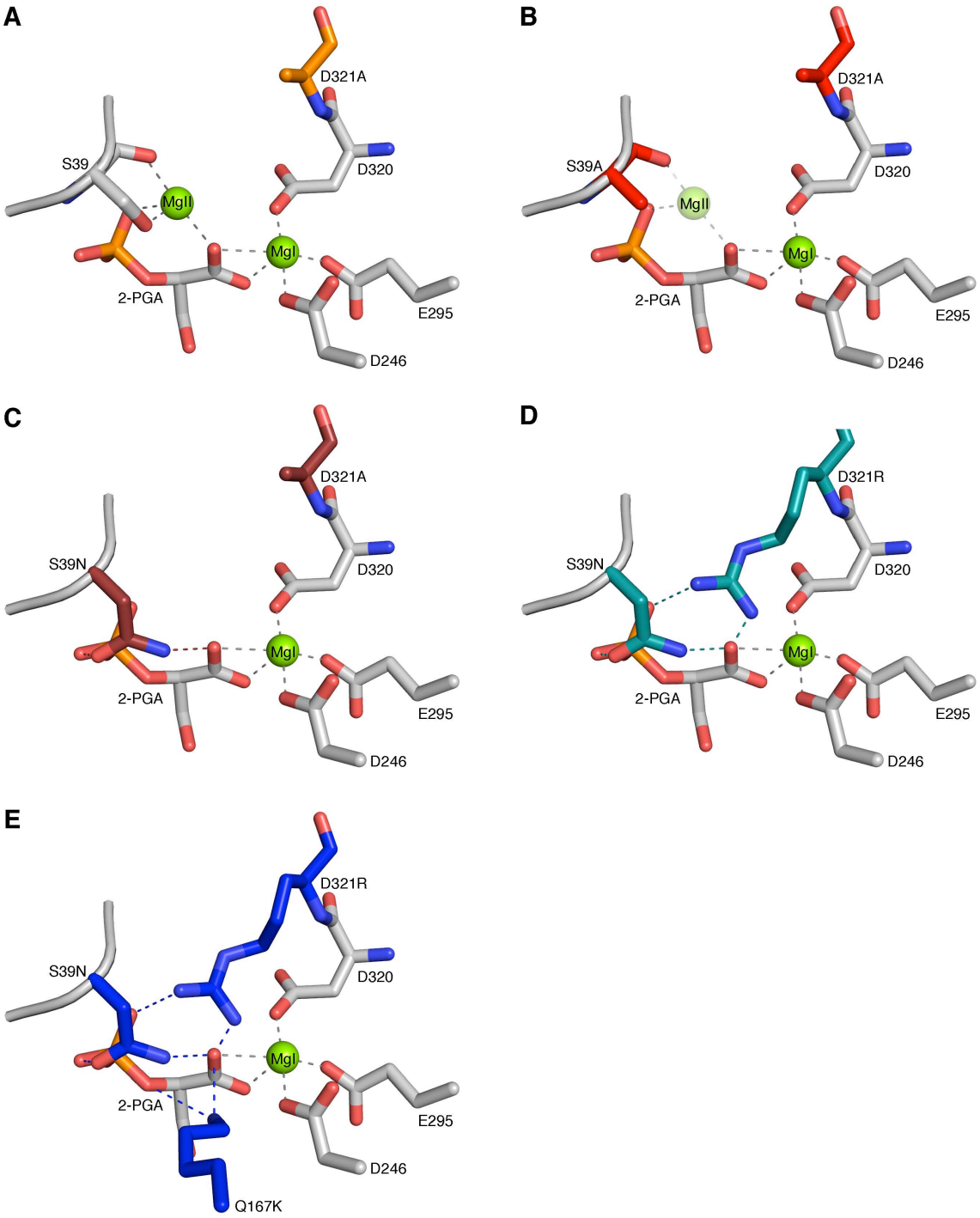


**Fig. S1:** Design of enolase mutants. (A) Predicted structure of the D321A active site with the D321A mutation (orange). As MgII retains most of its coordination sphere, we expected it to be present in the structure. (B) Predicted structure of the AA active site with the S39A and D321A mutations (red). MgII is depicted opaque, as it's coordination sphere is expected to be severely weakened due to the mutations. (C) Predicted structure

of the NA active site with the S39N and D321A mutations (dark red). The predicted rotamer of N39 interferes with MgII binding. (D) Predicted structure of the NR active site with the S39N and D321R mutations (teal). The predicted rotamers of N39 and R321 interfere with MgII binding. (E) Predicted structure of the NKR active site with the S39N, Q167K, and D321R mutations (blue). The predicted rotamers of N39, R321, and K167 interfere with MgII binding.

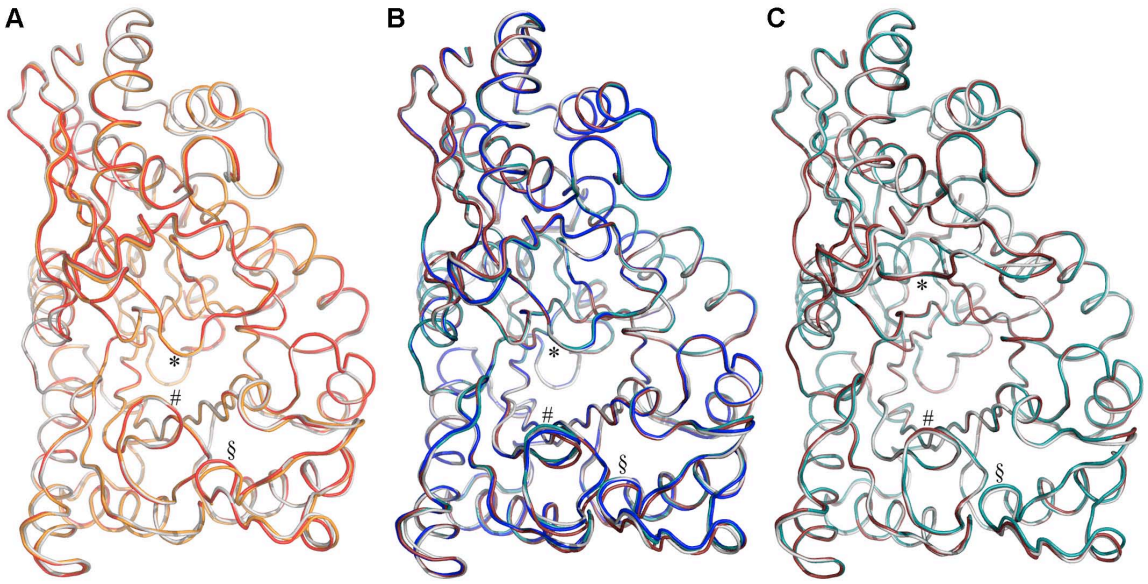


**Fig. S2:** Closed, open and apo conformations of enolase. In all structures * marks loop 36-43, # marks loop 153-169, and § marks loop 251-275. (A) Alignment of wild-type enolase (grey ribbon, PDB-entry 1one) in closed conformation with D321A (orange ribbon, rmsd of 0.28 Å over all Cα-atoms), and AA (red ribbon, rmsd of 0.27 Å over all Cα-atoms). (B) Alignment of enolase S39A (grey ribbon, PDB-entry 1l8p) in open conformation with NA subunit A (dark red ribbon, rmsd of 0.33 Å over all Cα-atoms), NR subunit A (deep teal ribbon, rmsd of 0.29 Å over all Cα-atoms), and NKR (blue ribbon, rmsd of 0.33 Å over all Cα-atoms). (C) Alignment of wild-type enolase (grey ribbon, PDB-entry 5enl) in apo conformation with NA subunit B (dark red ribbon, rmsd of 0.30 Å over all Cα-atoms), and NR subunit B (deep teal ribbon, rmsd of 0.25 Å over all Cα-atoms).

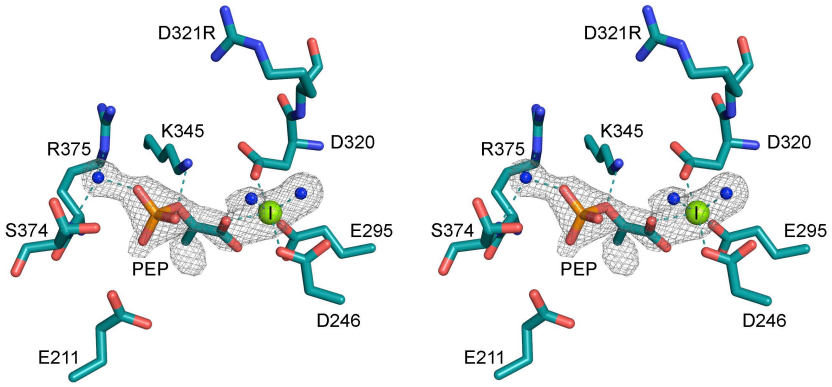


**Fig. S3:** Stereo image illustrating binding of PEP to the apo structure of enolase NR subunit B. The omit electron density ($F_o$-$F_c$) for PEP, MgI (green sphere) and the water molecules (blue spheres) is contoured at 3.0 σ (grey mesh). The less well-defined electron density of PEP indicates some flexibility in positioning of the ligand. S374 is flexible. In the precatalytic apo state, R321 is not coordinated to the substrate but points away from the active site. Catalytic contacts of PEP with K345 and E211 are not established.

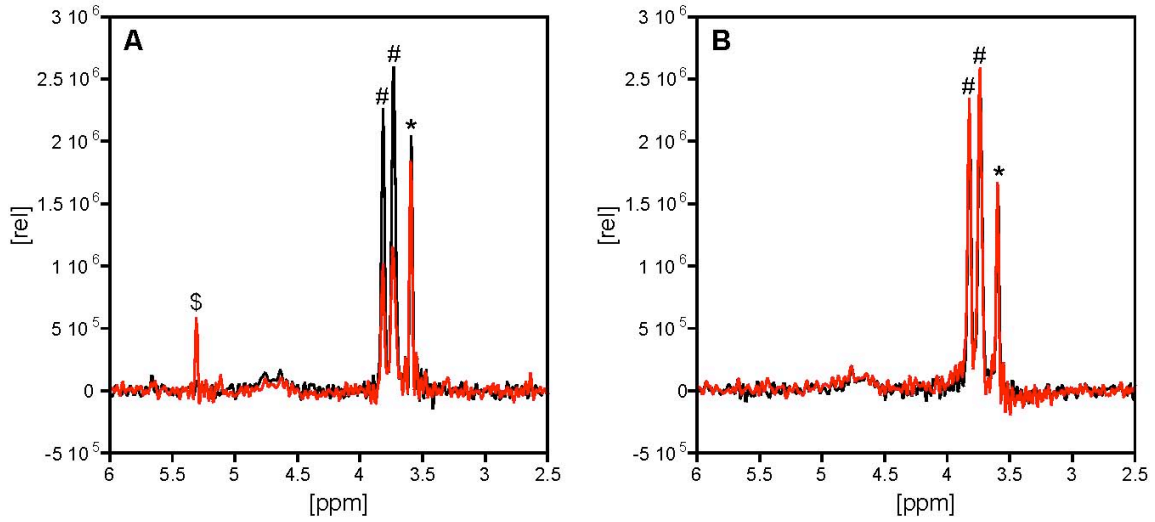


**Fig. S4:** $^{1}$H proton exchange measurements. In the spectra * marks buffer proton peak, # marks 2-PGA proton peaks, and $ marks PEP proton peak. (A) Spectra of assay solution before addition of enzyme (black) and after 45 min at 25 °C with 0.02 µM wild-type enolase added (red). After addition of active wild-type enolase the peaks of the 2-PGA protons are reduced while a new peak for the PEP protons appears. (B) Spectra of assay solution before addition of enzyme (black) and after two days at 25 °C with 0.5 µM NKR added (red). No significant change could be observed.

**Table S1:** Statistics for the D321A, NA, AA, NR, and NKR datasets.

| | **D321A** | **NA** | **AA** | **NR** | **NKR** |
|---|---|---|---|---|---|
| **Exp. Procedures** | | | | | |
| Crystallization buffer | 18 % PEG 6000, 0.2 M $MgCl_2$, 0.1 M Tris pH 8.0 | 20 % PEG 3350, 0.2 M $K_2SO_4$ | 18 % PEG 6000, 0.2 M $MgCl_2$ | 20 % PEG 8000, 0.2 M MgAc, 0.1 M NaCacodylate pH 6.5 | 25 % PEG 4000, 0.1 M NaAc pH 4.6 |
| Soaking solution | + 3.5 mM 2-PGA | + 3.5 mM 2-PGA, 3.5 mM $MgCl_2$ | + 3.5 mM 2-PGA | + 3.5 mM PEP, 3.5 mM $MgCl_2$ | + 3.5 mM PEP, 3.5 mM $MgCl_2$ |
| **Data collection** [$] | | | | | |
| Detector dist. (mm) | 140 | 130 | 100 | 110 | 200 |
| Wavelength (Å) | 1.000 | 0.979 | 1.000 | 0.979 | 0.827 |
| Spacegroup | P1 | P1 | P1 | P1 | P1 |
| Cell dimensions | a = 62.0 Å, b = 62.0 Å, c = 64.3 Å, α = 67.9 °, ß = 78.3 °, ɣ = 80.6 ° | a = 64.5 Å, b = 82.3 Å, c = 95.3 Å, α = 89.4 °, ß = 71.3 °, ɣ = 84.8 ° | a = 62.3 Å, b = 62.5 Å, c = 10.8 Å, α = 87.9 °, ß = 76.1 °, ɣ = 76.4 ° | a = 62.3 Å, b = 62.9 Å, c = 64.3 Å, α = 73.0 °, ß = 79.3 °, ɣ = 81.2 ° | a = 55.2 Å, b = 60.7 Å, c = 120.5 Å, α = 89.9 °, ß = 89.9 °, ɣ = 65.8 ° |
| No. of unique reflect. | 73,622 (11,719) | 162,601 (24,592) | 146,644 (23,385) | 64,875 (10,601) | 147,095 (22,243) |
| Redundancy | 1.81 (1.75) | 2.01 (1.77) | 2.01 (1.93) | 1.65 (1.63) | 1.97 (1.67) |
| Date range (Å) | 50.0-1.80 (1.91-1.80) | 40.0-1.79 (1.90-1.79) | 40.0-1.70 (1.80-1.70) | 40.0-1.80 (1.91-1.80) | 40.0-1.70 (1.80-1.70) |
| Completeness (%) | 91.3 (89.6) | 93.1 (87.3) | 92.4 (91.1) | 75.9 (76.8) * | 93.0 (86.9) |
| $R_{merge}$ (%) | 14.9 (68.2) | 12.6 (49.3) | 20.7 (82.7) | 16.1 (90.0) | 16.0 (77.1) |
| I/σ | 11.43 (3.12) | 12.74 (3.48) | 8.64 (2.65) | 11.66 (2.05) | 9.69 (2.34) |
| Wilson B value ($Å^2$) | 26.5 | 25.2 | 25.7 | 23.9 | 22.3 |
| **Refinement** [#] | | | | | |
| $R_{fact}$ (%) | 17.5 | 16.8 | 23.3 | 16.4 | 19.7 |
| $R_{free}$ (%) | 21.4 | 20.9 | 27.9 | 20.8 | 24.6 |
| Overall B value ($Å^2$) | 20.1 | 18.8 | 20.5 | 16.8 | 15.4 |
| Bond lengths rmsd (Å) | 0.007 | 0.011 | 0.016 | 0.010 | 0.011 |
| Bond angles rmsd (Å) | 1.071 | 1.181 | 1.603 | 1.245 | 1.315 |

| | | | | | |
|---|---|---|---|---|---|
| Dimers/assym. unit | 1 | 2 | 2 | 1 | 2 |
| No. of water molecules | 747 | 2567 | 1693 | 800 | 1596 |
| No. of atoms | 7292 | 14691 | 16055 | 7473 | 14910 |
| **Structure** | | | | | |
| Ligand | 2-PGA | 2-PGA | 2-PGA | PEP | PEP |
| MgII | present | missing | present (B), missing (A,C,D) | missing | missing |
| Loop 36-43 conf. | closed | open (A,C), apo (B,D) | closed (A,C), missing (B,D) | open (A), apo (B) | open |
| Loops 153-169 and 251-277 conf. | closed | open | closed | open | open |
| Overall state | closed (A,B) | open (A,C), apo (B,D) | closed (A,C), closed with loop 36-43 missing (B,D) | open (A), apo (B) | open (all) |
| Missing amino acids | 265 (A), His-tag (all) | His-tag (all) | 38-60 & 265 (B,D), His-tag (all) | His-tag (all) | His-tag (all) |
| Ramachandran outliers | R402 (all) | R402 (all) | R402 (all) | R402 (all) | R402 (all) |
| Cis-peptides | 142-143 (all) | 142-143 (all) | 142-143 (all) | 142-143 (all) | 142-143 (all) |

[$] In the data collection statistics the numbers given in brackets correspond to the values of the last shell. [#] In the structure statistics, names of different subunits in the crystals are given in brackets. * The NR dataset contained ice rings, thus certain resolution ranges had to be excluded from the calculations, resulting in lower overall completeness.